Electronic Journal of Biotechnology 51 (2021) 40–49

Contents lists available at ScienceDirect

Electronic Journal of Biotechnology

journal homepage:

Research Article

Molecular characterization and functional analysis of scavenger receptor class B from black tiger shrimp (*Penaeus monodon*)

Sigang Fan [a], Fang Wang [a], Zhuofang Xie [a], Chao Zhao [a], Pengfei Wang [a], Lulu Yan [a], Xufeng Wang [a], Youhou Xu [b], Lihua Qiu [a,c,*]

[a] *Key Laboratory of Aquatic Product Processing, Key Laboratory of South China Sea Fishery Resources Exploitation & Utilization, Ministry of Agriculture, South China Sea Fisheries Research Institute, Chinese Academy of Fishery Sciences, Guangzhou, PR China*
[b] *Guangxi Key Laboratory of Beibu Gulf Marine Biodiversity Conservation, Beibu Gulf University, Qinzhou, PR China*
[c] *Key Laboratory of Aquatic Genomics, Ministry of Agriculture, PR China*

ARTICLE INFO

Article history:
Received 3 July 2020
Accepted 16 March 2021
Available online 29 March 2021

Keywords:
Astaxanthin
Binding
Black tiger shrimp
Carotenoid
HPLC
Molecular characterization functional analysis
Multifunctional protein
Penaeus monodon
Pigment
Scavenger receptors
Transcriptome

ABSTRACT

Background: Scavenger receptor class B (SRB) is a multifunctional protein in animals that participates in physiological processes, including recognition of a wide range of ligands. Astaxanthin is a major carotenoid found in shrimp. However, the molecular mechanism of astaxanthin and SRB protein binding has not been reported.

Results: In the present study, a member of the *SRB* subfamily, named *PmSRB*, was identified from the transcriptome of black tiger shrimp (*Penaeus monodon*). The open reading frame of *PmSRB* was 1557 bp in length and encoded 518 amino acids. The structure of PmSRB included a putative transmembrane structure at the N-terminal region and a CD36 domain. Multiple sequence alignment indicated that the CD36 domain were conserved. Phylogenetic analysis showed four separate branches (SRA, SRB, SRC, and croquemort) in the phylogenetic tree and that PmSRB was clustered with SRB of *Eriocheir sinensis*. Quantitative real-time polymerase chain reaction showed that the *PmSRB* gene was widely expressed in all tissues tested, with the highest expression level observed in the lymphoid organ and brain. Subcellular localization analysis revealed that PmSRB-GFP (green fluorescent protein) fusion proteins were predominantly localized in the cell membrane. The recombinant proteins of PmSRB showed binding activities against astaxanthin *in vitro*.

Conclusions: *PmSRB* was identified and characterized in this study. It is firstly reported that PmSRB may take as an important mediator of astaxanthin uptake in shrimp.

How to cite: Fan S, Wang F, Xie Z, et al. Molecular characterization and functional analysis of scavenger receptor class B from black tiger shrimp (*Penaeus monodon*). Electron J Biotechnol 2021; 51. https://doi.org/10.1016/j.ejbt.2021.03.003

1. Introduction

Carotenoids are a group of fat-soluble, plant-derived pigment molecules that mostly animals cannot synthesize *de-novo*, and therefore must be obtained exclusively from their diet [1]. In mammals and birds, carotenoids are first released from the food matrix in the gut, solubilized into mixed micelles and absorbed by intestinal mucosal cells [2]. Then, carotenoids were transported in the circulation, and delivered to target tissues (such as retina, epidermal tissue), and finally, in some cases, metabolized [2,3]. In Atlantic salmon *Salmo salar*, carotenoids are ingested in midgut and deposited in flesh [3]. In silkworm *Bombyx mori*, carotenoids are absorbed into the midgut epithelium, transferred to hemolymph lipoprotein, lipophorin, and deposited in the middle silk gland [4]. In crustaceans, carotenoids such as canthaxanthin, lutein or zeaxanthin could be metabolized into astaxanthin in internal organ [5].However, there has been very little progress on the biochemical pathway of carotenoid metabolism in crustaceans [5]. Carotenoids are highly hydrophobic and therefore require special transport by lipoproteins through plasma (or hemolymph) to tissues for deposition [6]. The process of carotenoids accumulated in the retina is likely supported by zeaxanthin-binding protein [7]. In addition, scavenger receptors (SRs) may recognize carotenoids and facilitate the movement of it into the cell [3].

Peer review under responsibility of Pontificia Universidad Católica de Valparaíso
* Corresponding author.
E-mail address: qiugroup_bio@outlook.com (L. Qiu).

https://doi.org/10.1016/j.ejbt.2021.03.003
0717-3458/

Scavenger receptors are a large superfamily of membrane-bound receptors that can bind to and endocytose a vast range of ligands, modified low-density lipoproteins, bacteria, and apoptotic cells [8]. SRs are comprised of a diverse array of integral membrane proteins and soluble secreted extracellular domain isoforms [9]. In recent years, SRs have been classified into 10 eukaryote families (i.e., A–J) based on their structure and biological function [10]. Seven classes, from A to H (excluding C), have been recognized in mammals, whereas only two discrete classes, SRB and SRC, have been characterized in *Drosophila* [11]. Gene products from SRBs contain a central domain of ~400–450 residues that are glycosylated. SRBs have two transmembrane regions located close to the N- and C-terminals, which play regulatory roles in signal transduction and trafficking [9]. In mammals, four SRB members have been identified, including SRB1, SRB2, SRB3, and lysosomal integral membrane protein 2 (LIMP2). SRBs have been implicated as carotenoid transporters in lower species and in various tissues of higher animals [12–15]. In humans, three SRBs (SRB1, SRB2, and CD36) are capable of binding and transporting macular xanthophyll carotenoids [12]. In silkworm *B. mori*, SCRB15 is involved in selective b-carotene movement and Cameo2 (homologous to mammalian SCARB1) can enhance selective lutein transport [13]. In *Drosophila melanogaster*, NinaD (homologous to CD36 and SRB1 in vertebrates) is essential for cellular uptake of carotenoids [16]. In addition, SRB1 is an important mediator of carotenoid-based coloration [3]. For example, genetic variation screening in Atlantic salmon (*S. salar*) identified a novel paralog of SRB1 (i.e., SCARB1) in a region containing a putative quantitative trait locus (QTL) for flesh color [17]. Transcriptome analysis of noble scallop also revealed a novel scavenger receptor (SRB-like-3), which is likely associated with orange scallop carotenoid content. Lei et al. [18] found that SRB may be involved in the absorption of carotenoids in the pearl oyster.

Astaxanthin is a major carotenoid found in a variety of aquatic animals, including crustaceans [19]. Astaxanthin is used as feed additives in shrimp farming to ensure a bright red or pink appearance in crustacean and salmonidae species, with such animals considered to be of higher quality [2,20]. In crustaceans, astaxanthin plays a role in pigmentation, antioxidation, and photoprotection, and is a source of provitamin A [20]. Astaxanthin is reported to be the predominant carotenoid in five commercial shrimp species (*P. monodon*, *Fenneropenaeus chinensis*, *Litopenaeus vannamei*, *Exopalaemon carinicauda* and *Trachypenaeus curvirostris*) [21]. In addition, Zhang et al. [22] found high concentrations of free astaxanthin in a new variety of ridgetail white prawn. However, the mechanisms of carotenoid uptake and transport are not well understood in animals. At present, only a few proteins that can bind to astaxanthin have been reported [23,24]. For example, within the exoskeleton and hypodermal tissue of crustaceans, two crustacyanin (CRCN) proteins are known to bind with two astaxanthin molecules, which then dimerize to form β-crustacyanin [24]. Lower *CRCN-A* and *CRCN-C* expression and total astaxanthin levels are found in albino shrimp (*F. merguiensis*) than in light or dark shrimp [25]. Lipocalin (a CRCN homologue) knockdown in freshwater shrimp (*Macrobrachium rosenbergii*) results in a body color change from blue to orangish red [26]. Furthermore, lipocalin can bind to astaxanthin *in vitro* [26]. Several *SRB* genes have been discovered in crustaceans, which play important roles in host defense against microbial pathogens [27,28]. However, the role of SRBs in astaxanthin uptake has not been reported.

P. monodon is an economically important aquacultural species, with a global production of 739,426 tons and output value of $US5.6 billion [29]. Carotenoid content in *P. monodon* (32.23 mg/kg fresh muscle) is higher than that in *L. vannamei* (2.12 mg/kg) and *F. chinensis* (2.22 mg/kg) [21]. More than 80% of carotenoid content in *P. monodon* muscle is astaxanthin [21]. Astaxanthin is easily absorbed through the digestive tract and is preferentially deposited in the flesh [30]. However, the molecular mechanism of astaxanthin and protein binding remains poorly understood.

In the present study, the cDNA sequence of the *SRB* gene (*PmSRB*) in *P. monodon* was cloned and characterized. Sequence alignment was performed, and a phylogenetic tree was constructed. To elucidate *PmSRB* function, we examined mRNA expression profiles in various tissues, investigated the binding ability of PmSRB recombinant protein to astaxanthin *in vitro*, and detected its cellular localization. Our results provide some insight into the functions and molecular mechanisms of *PmSRB* in astaxanthin binding. Astaxanthin is an important antioxidant in humans, and target breeding and consumption of shrimp with high astaxanthin content may be of benefit.

2. Materials and methods

2.1. Experimental animals

Ten adult tiger shrimp (weight 200 ± 2 g) were purchased from the Huangsha Aquaculture Market, Guangzhou, Guangdong Province, China. The shrimp were cultured in a tank (500 L) with aerated seawater for 3 d before experimental analyses. The temperature and salinity of the sea water were maintained at 26 ± 2°C and 3.3%, respectively. Two-thirds of the seawater was changed every day. The shrimp were fed commercial pellets (Xiaduokang, HAID, Guangdong, China) until 24 h prior to the experiment. Five healthy shrimp were chosen randomly. Tissue samples, including gill, stomach, muscle, hepatopancreas, brain, lymphoid organ, and intestine, were dissected with sterilized scissors, then collected in sterile tube and stored in liquid nitrogen and frozen in liquid nitrogen, and stored at −80°C until use.

2.2. Total RNA extraction and cDNA synthesis

Total RNA was extracted from tissues using a TRIzol RNA isolation kit (Invitrogen, USA) according to the manufacturer's instructions. Total RNA quality was examined by 1.0% agarose gel electrophoresis and a NanoDrop-2000 (Thermo Fisher, USA). The first strand cDNA synthesis was carried out using 1 μg of total RNA from muscle and a Prime Script II 1st strand cDNA synthesis kit (TaKaRa, Japan). For quantitative real-time PCR (qRT-PCR), total RNA from tissue samples such as muscle, hepatopancreas, brain et al, were used as the template for the RT-reaction based on a PrimeScript™ RT reagent kit with gDNA Eraser (TaKaRa, Japan), respectively.

2.3. Sequence analysis of PmSRB cDNA

Full-length cDNA of *PmSRB* was obtained from the transcriptome of *P. monodon* (data not published). Sequence accuracy was confirmed by PCR using a pair of primers SRB-F/R (Table 1). PCR was performed in a 20 μl reaction volume, containing 2 μl 10 ×Ex Taq buffer (Mg^{2+} plus) (TaKaRa), 0.8 μl of each primer (10 μM), 0.2 μl ExTaq (5 U/μl), 1.6 μl dNTP mixture (2.5 mM each), 1.0 μl cDNA, and 13.6 μl ddH_2O. The PCR program was 1 cycle at 95°C for 5 min, 35 cycles at 95°C for 30 s, 60°C for 30 s, and 72°C for 30 s, and finally 1 cycle at 72°C for 5 min. The obtained DNA fragments were purified with SanPrep Column DNA Gel Extraction Kit (Sangon, China), cloned with pMD™ 18-T Vector Cloning Kit (TaKaRa, Japan), and finally sequenced by the dideoxy method of Sanger in Sangon Biotech Company in Shanghai, China.

The similarity between *PmSRB* and other genes was analyzed using the BLAST algorithm in the NCBI database (http://www.ncbi.nlm.nih.gov/blast/). The ORF Finder (http://www.ncbi.nlm.

Table 1
Primers used in this research.

Primer	Sequence (5′→3′)	Purpose	Product size (bp)
SRB-F	ATGCGCAGAATACAGTGTGC	cDNA cloning	1557
SRB-R	TCATGCTGCATCTTTATCCC	cDNA cloning	
qSRB-1-F	GTGTAGGAGGTCCACCATGC	qRT-PCR	144
qSRB-1-R	GGTCTGGCTTCATTCCGACA	qRT-PCR	
EF-1α-F	AAGCCAGGTATGGTTGTCAACTTT	qRT-PCR	73
EF-1α-R	CGTGGTGCATCTCCACAGACT	qRT-PCR	
O-SRB-F	CGCGGATCCgaattcGATTTTATCAACCAAATCAT	Recombinant protein expression	1233
O-SRB-R	TGCGGCCGCaagcttTTTTGTCACCTCTGGTACAT	Recombinant protein expression	
GFP-SRB-F	CTCGAGCTCaagcttATGCGCAGAATACAGTGTGC	Subcellular location	1554
GFP-SRB-R	GCGACCGGTggatccCGTGCTGCATCTTTATCCCCGT	Subcellular location	

Note: Lower case letters represent restriction enzyme sites. F, forward; R, reverse.

nih.gov/gorf/gorf.html) and Translate programs (http://web.expasy.org/translate) were used to obtain the open reading frames (ORFs) and to predict the coding protein sequence, respectively. The physical and chemical properties of proteins were predicted by ProtParam (http://web.expasy.org/protparam/). SMART (http://smart.embl-heidelberg.de/smart/) was used for analysis of the functional domains of the deduced protein sequences. TMHMM (http://www.cbs.dtu.dk/services/TMHMM-2.0/) and SignalP (http://www.cbs.dtu.dk/services/SignalP/) were used to predict the transmembrane structure and signal peptide of the deduced protein, respectively. Potential N-linked glycosylation sites were predicted according to the Asn-X-Ser/Thr rule (http://cbs.dtu.dk/services/NetNGlyc). Multiplex sequence alignment was performed using Clustalw2 software. A phylogenetic tree was created with MEGA 6.06 based on amino acid sequence alignments using the neighbor-joining (NJ) algorithm, with branching reliability evaluated by the bootstrap method with 1000 pseudoreplicates.

2.4. Quantitative real-time PCR (qRT-PCR)

The relative expression levels of *PmSRB* in different tissues were analyzed using qRT-PCR. cDNA was diluted to 1:10 with ddH_2O and stored at −20°C. Specific primers were designed using the *PmSRB* cDNA sequence, and elongation factor-1α (*EF-1α*) (GenBank No. DQ021452.1) was selected as the reference gene [24] (Table 1). qRT-PCR was conducted using the LightCycler® 480II RT-PCR System (Roche, America). PCR was performed in a 13-μl reaction volume, containing 6.5 μl of 2 × TB Green Premix Ex Taq (Tli RNaseH Plus) (TaKaRa, Japan), 0.5 μl of each primer (10 μM), 1.0 μl of cDNA, and 4.5 μl of RNase-free water. The PCR cycling program consisted of denaturation at 95°C for 30 s, 40 cycles at 95°C for 5 s and 60°C for 40 s. To assess the specificity of the PCR amplification, a melting curve step (95°C for 1 s, 60°C for 20 s and 95°C for 1 s) was obtained at the end of the reaction, and a single peak was observed. Each assay was performed in triplicate. The qRT-PCRs were repeated in a minimum of three independent experiments. The comparative C_T method ($2^{-\Delta\Delta CT}$) was used to analyze relative expression levels [31]. The amplification efficiencies of the target and reference genes were verified and found to be approximately equal.

2.5. Recombinant expression and purification of CD36 domain of PmSRB

The fragment encoding the CD36 domain was amplified with primers O-SRB-F and O-SRB-R (Table 1). PCR was performed in a 20 μl reaction volume, containing 2 μl 10 × Ex Taq buffer (Mg^{2+} plus) (TaKaRa, Japan), 0.8 μl of each primer (10 μM), 0.2 μl ExTaq (5 U/μl),1.6 μl dNTP mixture (2.5 mM each), 1.0 μl cDNA, and 13.6 μl ddH_2O. The PCR program was 1 cycle at 95°C for 5 min, 35 cycles at 95°C for 30 s, 56°C for 30 s, and 72°C for 1 min, and finally 1 cycle at 72°C for 7 min. For the convenience of cloning, an *Eco*R I site was added to the 5′ end of primer O-SRB-F and a *Bam*H I site was added to the 5′ end of primer and then inserted into the same restriction enzyme sites of expression vector pET-28a (Invitrogen, USA). The recombinant plasmid (pET-28a-PmSRB) was transformed into *Escherichia coli* Rosetta (DE3) (TransGen, China), and the positive clones were collected and sequenced.

The positive transformants were incubated overnight (37°C, 200 rpm) in Luria-Bertani (LB) medium (50 μg/mL kanamycin). An aliquot of the culture (400 μL) was transferred to 40 mL of fresh LB medium. When the OD_{600} of the culture reached 0.6, isopropyl β-D-1-thiogalactopyranoside (IPTG) was added to the LB medium at a final concentration of 0.1 mmol/L for 8 h (30°C, 130 rpm). Bacteria were harvested by centrifugation at 10,000 g for 10 min at room temperature. The resulting cell pellet was resuspended in NTA-0 (12.11 g Tris base, 146.1 g NaCl, 500 mL glycerinum, 6 mL concentrated hydrochloric acid, added ddH_2O to final volume 5 L), followed by the addition of lysozyme (10 mg/ml) on ice for 30 min. After breaking by ultrasound, the bacterial lysate was centrifuged at 16,000 rpm for 50 min at room temperature.

The sediment was suspended in STET buffer (100 mM Sodium Chloride; 10 mM Tris-HCL; 1 mM EDTA; and 5% Triton X-100), with dithiothreitol (DTT) then added at a final concentration of 1 mmol/L. The solution was broken by ultrasound and centrifuged at 10,000 rpm for 10 min at 4°C. The sediment was suspended in phosphate-buffered saline (PBS). After again breaking by ultrasound and centrifugation at 10,000 rpm for 10 min at 4°C, the sediment was suspended in 3 mL of guanidine hydrochloride, with DTT added at a final concentration of 5 mmol/L. The inclusion body was dissolved by shaking at 10,000 rpm for 10 min at 4°C and then diluted with guanidine hydrochloride (3 M). This solution was added by drops and then stirred into refolding buffer (40 mL, 50 mM Tris–HCl pH 8.0 containing 0.15 M NaCl, 1 mM EDTA, 0.5 M L-arginine, 2 mM reduced glutathione, 1 mM oxidized glutathione, and 5% (v/v) glycerol) for 24 h. The resulting solution was dialyzed against a TE buffer and then concentrated using polyethylene glycol (PEG) 20,000 to 10–20 mL. All procedures were performed at 4°C. The recombinant PmSRB (rPmSRB) protein was purified using a Ni-NTA Sepharose column (Invitrogen, USA). The resulting concentrations of the PmSRB protein were measured using a modified BCA protein assay kit (Sangon Biotech, China). The purified recombinant proteins were stored at −80°C for subsequent experiments.

2.6. Western blotting analysis to detect PmSRB protein

In western blot analysis, rPmSRB was separated by SDS–PAGE (15% separation gel and 5% concentrated gel) and electrophoretically transferred onto nitrocellulose membranes. The membranes were blocked by incubation in 5% skim milk powder solution at 37°C for 2 h. After washing in PBST (0.05% Tween 20 in PBS) three

times (5 min each time), the membranes were incubated with 1:1000 (v/v) anti-mouse His at 37°C for 1 h, then washed with PBST three times, and incubated with 1:10,000 (v/v) horseradish peroxidase-conjugated goat anti-mouse IgG (Jackson Immuno Research, America) with gentle shaking at 37°C for 1 h. Finally, the membranes were washed three times with PBST for 10 min each, and then immersed in an electrochemiluminescence (ECL) luminescence reagent (Sangon, China) (combining solutions A and B of the ECL kit in a 1:1 ratio) with agitation for 1 min. After washing, the blots were developed by ECL.

2.7. In vitro binding assay

1 mg astaxanthin (Sigma, America) was diluted with 1 mL of dimethyl sulfoxide (DMSO). Then 30 μl astaxanthin solution and 200 mL of rPmSRB (1 mg/ml) were incubated with 5 mL nondenature lysis buffer (50 mM NaH_2PO_4, 300 mM NaCl) at room temperature for 2 h. The rPmSRB-astaxanthin complexes were collected with 100 mL of His-tag purification resin (Beyotime, China). The resin was washed five times with 0.5 mL of nondenature washing buffer (50 mM NaH_2PO_4, 300 mM NaCl and 2 mM imidazole). The protein-astaxanthin complexes were eluted in 0.5 mL of nondenature elution buffer (50 mM NaH_2PO_4, 300 mM NaCl and 50 mM imidazole) 6–10 times. Acetone (5 mL) was used to extract astaxanthin from eluent. After drying with a Termovap Sample Concentrator (Organomation, USA), astaxanthin was resuspended in 5 mL of methanol for high-performance liquid chromatography (HPLC) analysis. HPLC analysis using an Agilent 1200 HPLC system (Agilent Technologies Inc., USA). A Shimadzu LC-C18 column Agilent Technologies Inc., USA) was used for HPLC analysis. The eluting conditions were 95% methanol. The flow rate was 1.0 mL/min and column temperature was 25°C. Astaxanthin standard solution (0.01 mg/ml) was used as a control. The detecting wavelength was set between 300 and 650 nm, and the chromatographic peaks were measured at a wavelength of 480 nm to facilitate the detection of astaxanthin. All assay were repeated 3 times. Astaxanthin standard solution (0.01 mg/ml) was used as a control.

2.8. Subcellular localization

The full-length ORFs of the *PmSRB* genes were amplified from *P. monodon* cDNA by PCR using a pair of primers (GFP-SRB-F and GFP-SRB-R) (Table 1). PCR-product cleavage was carried out with *Hind* III and *Bam*H I (TaKaRa, Japan) and cloned into pEGFP-N1 (Invitrogen, USA). The recombinant plasmids were transferred into *E. coli* DH5α and then extracted from DH5α with an Endo-free Plasmid Mini Kit (Promega, USA) according to the manufacturer's instructions. The constructed recombinant plasmids were subsequently verified by DNA sequencing.

HEK293T cells (Obio Technology Corp., Ltd., Shanghai, China) were cultured in DMEM (Thermo Fisher, USA) supplemented with 10% fetal bovine serum (FBS) (Invitrogen, USA) and antibiotics (10^5 U/L penicillin and 100 mg/L streptomycin, Gibco, USA) at 37°C in a humidified incubator under 5% CO_2. For transfection of empty vector pEGFP-N1 and for combined expression of vector pEGFP-N1-PmSRB, HEK293T cells were allowed to grow to more than 70% confluence, followed by plasmid transfection using Lipofectamine 3000 (Invitrogen, USA) according to the manufacturer's instructions.

Culture medium was removed at 24 h post-transfection, and the cells were washed with PBS and fixed with 10% (v/v) neutral buffered formalin for 10 min. After washing, cells were treated with PBST (2 mM KH_2PO_4, 8 mM Na_2HPO_4, 10 mM KCl, 140 mM NaCl and 0.05% Tween-20) for 10 min and then stained with 1 μg/mL Hoechst (Beyotime, China) for 10 min. Coverslips were washed with PBS. Finally, cellular localization of the PmSRB protein was observed using a Leica TCS SP5 laser confocal microscope (Leica, Germany).

3. Results

3.1. Cloning and sequence analysis of PmSRB

The complete cDNA sequence of *PmSRB* was obtained and deposited in GenBank under accession number MN928530. The full-length cDNA of *PmSRB* was 2329 bp with 5′-UTR of 113 bp, 3′-UTR of 659 bp, and ORF of 1557 bp (Fig. 1). The *PmSRB* gene encoded a protein sequence of 518 amino acid residues, with an estimated molecular mass of 58.06 kDa and an isoelectric point (pI) of 5.66. Sequence analysis indicated that *PmSRB* had a putative transmembrane structure (7–29 aa) in the N-terminal region. The result of transmembrane region predicted showed that the proba-

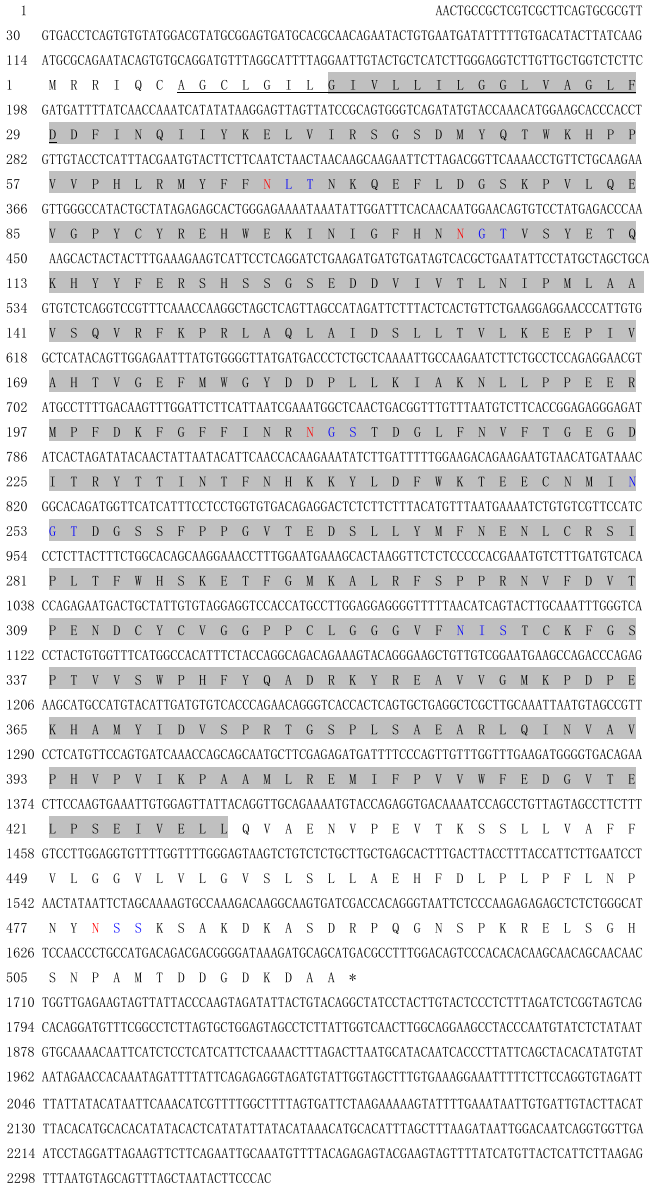

Fig. 1. Nucleotide and deduced amino acid sequences of *Penaeus monodon*. Amino acid sequences are shown under cDNA sequences. Transmembrane segment is underlined. CD36 domain is shaded in dark gray. Six Asn-Xaa-Ser/Thr sequons in sequence output are in blue. Four asparagines predicted to be N-glycosylated are in red.

bility of the transmembrane region appearing in the C-terminal was above 70%. The CD36 domain, a characteristic domain of the SRB protein family, was observed from the N-terminal region to C-terminal region (14–429 aa) of PmSRB. In addition, six Asn-Xaa-Ser/Thr sequons and four predicted N-linked glycosylation sites were detected in the amino acid sequence of PmSRB (Fig. 1). The NCBI BLASTP program revealed that the predicted amino acid sequence showed a homology match with a variety of SRBs previously registered to GenBank. BLASTP analysis of PmSRB showed 61% and 34% identity with *Eriocheir sinensis* SRB (GenBank No. AUM57516.1) and *Homo sapiens* SRB (GenBank No. NP_001076428.1), respectively. Multiple sequence alignment showed that all 41 single conserved residues (denoted as "*") and 92.65% strong conserved residues (denoted as ":") were found in the CD36 domain (Fig. 2). Three N-linked glycosylation sites (the 67th, 104th and 209th amino acid in PmSBB protein sequence) located in CD36 domain were conserved and shaded in yellow (Fig. 2). These results show that CD36 domain is conserved.

Fig. 2. Multiple alignment of PmSRB amino acid sequences with those of SRB from other species. Accession numbers of SRB genes from GenBank are as follows: RnSRB (*Rattus norvegicus* BAA14004.1); PmSRB (*Penaeus monodon* MN928530); EsSRB (*Eriocheir sinensis* AUM57516.1); SiSRB (*Solenopsis invicta* XP_025994337.1); SsSRB (*Salmo salar* NP_001117084.1); PtSRB (*Portunus trituberculatus* AMY96569.1); PpSRB (*Penaeus penicillatus* QCQ82556.1); SpSRB (*Scylla paramamosain* SKB10748.3); MmSRB (*Mus musculus* XP_017176253.1); DrSRB (*Danio rerio* XP_017213429.1); PjSRB (*Penaeus japonicus* BAJ10664.1); BmSRB (*Bombyx mori* NP_001164650.1); CcSRB (*Cyprinus carpio* QFZ79187.1); CD36 domain is represented with an underline. Three conserved N-linked glycosylation sites are shaded in yellow. Markers "*", ":", and "." indicate positions with single, strong, or weakly conserved residues, respectively.

A phylogenetic tree was constructed using the deduced amino acid sequences of SRA, SRB, SRC, and croquemort in invertebrates and vertebrates (Fig. 3). The amino acid sequences from different species were clustered into four separate branches (i.e., SRA, SRB, SRC, and croquemort). Furthermore, based on the phylogenetic tree, the PmSRB and *E. sinensis* SRB protein showed a close relationship.

3.2. Tissue expression of PmSRB transcripts

The tissue distribution pattern of *PmSRB* mRNA is shown in Fig. 4. The qRT-PCR results indicated that the *PmSRB* gene was expressed in all examined tissues, with relatively high levels observed in the lymphoid organ and brain and relatively low levels detected in the gill, muscle, hepatopancreas, stomach, and intestines (Fig. 4). The expression of *PmSRB* in lymphoid organ was 20-fold of that in the muscle, 23-fold, 82-fold, 130-fold and 138-fold of that in the hepatopanceas, stomach, gill and intestine, respectively. The expression of *PmSRB* in brain was 18-fold of that in the muscle, 20-fold, 72-fold, 114-fold and 121-fold of that in the hepatopanceas, stomach, gill and intestine, respectively.

3.3. PmSRB localization in cell membrane

Subcellular localization of PmSRB was investigated by green fluorescent protein (GFP) fusion protein expression in HEK293T cells. In the PmSRB-GFP fusion protein-transfected HEK293T cells, green fluorescence signals were predominantly observed in the cell membrane (Fig. 5, upper row). In the pEGFP-N1-transfected cells, fluorescence signals were primarily observed in the cytoplasm and nucleus (Fig. 5, lower row).

3.4. Expression, purification, and western blotting of rPmSRB protein

The CD36 domain of PmSRB was expressed in *E. coli* Rosetta with the pET28a system. The recombinant expressed protein was induced by IPTG and detected by 15% SDS–PAGE and western blot analysis. In contrast to non-induced *E. coli* (Fig. 6, lane 2), a thick band (Fig. 6, lane 1) was observed at the molecular weight of 49 kDa, indicating that rPmSRB was expressed successfully. rPmSRB was detected in the inclusion body (Fig. 6, lane 4), but not in the supernatant (Fig. 6, lane 3). rPmSRB was purified (Fig. 6, lane 5). Through stepwise dialyses, rPmSRB was refolded and obtained successfully (Fig. 6, lane 6). Western blot analysis showed that one specific target protein (Fig. 6, lane 7), which showed that it was consistent with the predicted molecular mass.

3.5. In vitro ligand binding assay

The rPmSRB was incubated with astaxanthin, with the resulting complex then analyzed by HPLC. Results showed that rPmSRB was specifically associated with astaxanthin (Fig. 7). The astaxanthin peak was observed at 7.42 s in each group. In the astaxanthin standard group, the peak area was 1717.4 and the peak height was 90.7 mAU. In the rPmSRB-astaxanthin complex group, the peak area was 179.2 and the peak height was 9.9 mAU. Based on peak area and the concentration of astaxanthin and rPmSRB, 1 mol of PmSRB could bind to 0.48 mol of astaxanthin.

4. Discussion

SRBs are type III transmembrane receptors, which consist of a transmembrane region, CD36 domain, and cytoplasmic tail [8]. SRBs participate in the recognition of a broad range of polyanionic ligands, including those found in high/low-density lipoproteins,

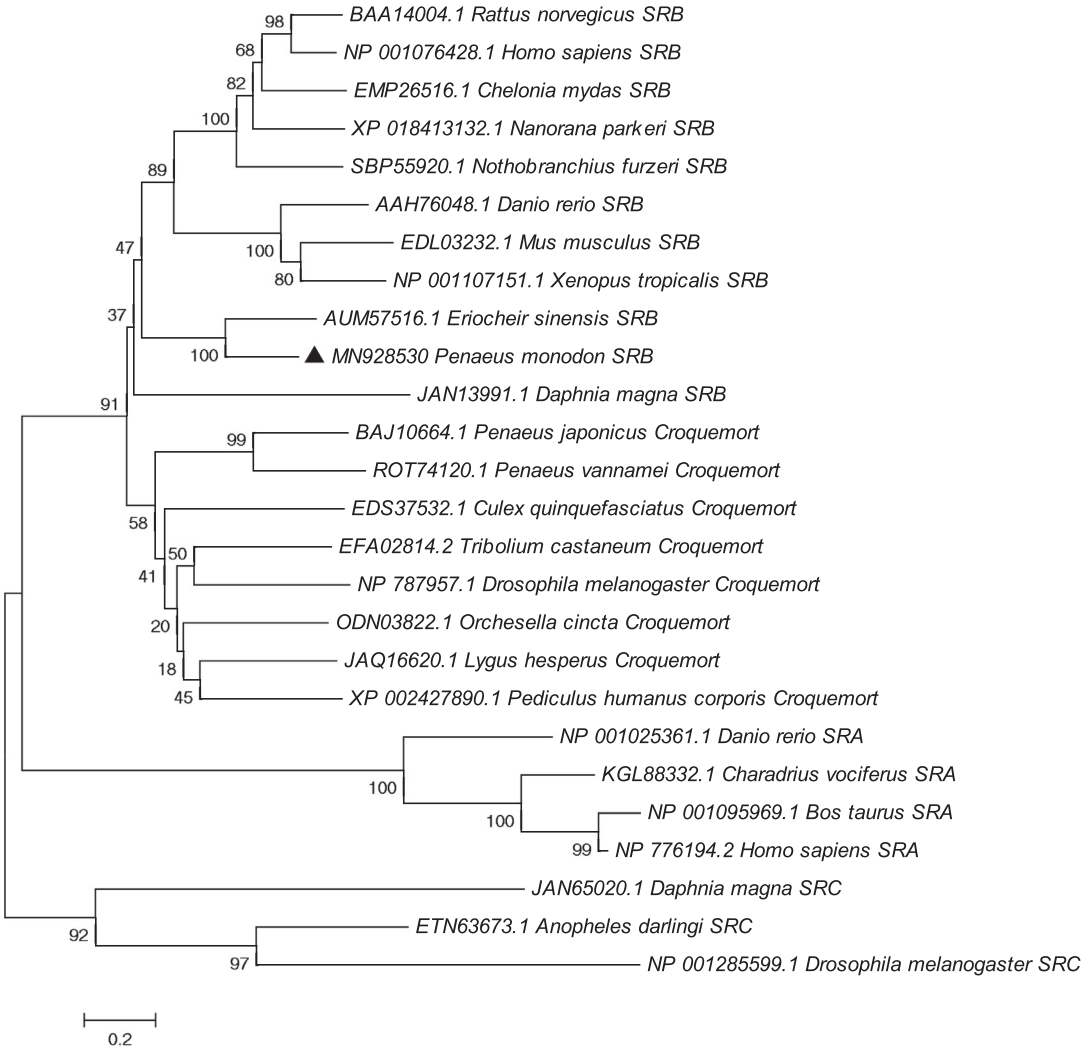

Fig. 3. Phylogenetic tree of SR proteins. SRB, SRA, SRC, and Croquemort molecules from various species were included for phylogenetic analysis. The black triangle (▲) indicates *Penaeus monodon* SRB.

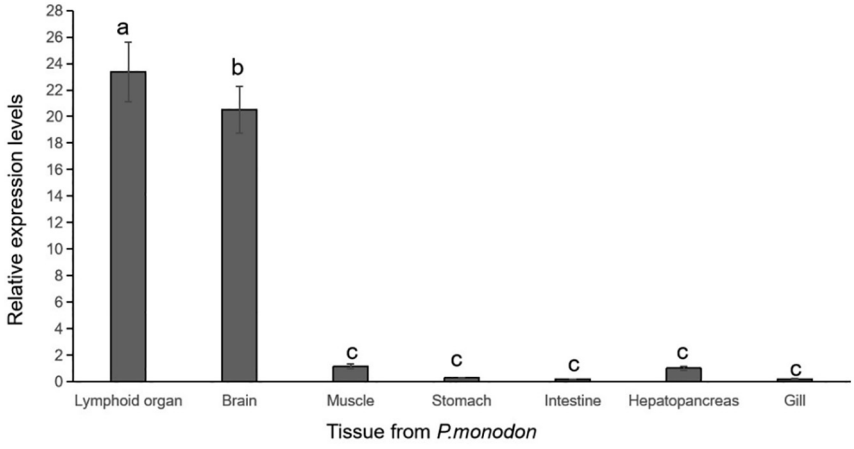

Fig. 4. Expression of *PmSRB* mRNA in different tissues of *P. monodon*. Significant differences are indicated by different letters ($P < 0.05$). Error bars correspond to mean + SE ($n = 5$).

bacteria, and apoptotic cells [12,32]. In this study, a novel SRB with the ability to bind to astaxanthin was cloned and characterized from *P. monodon*. As found in other SRBs from *Drosophila*, humans, birds, fish, and crustaceans, a CD36 domain was also predicted in the PmSRB protein [9,14,16,17,27,28]. Multiple sequence alignment showed that the CD36 domains of SRB are conserved in a

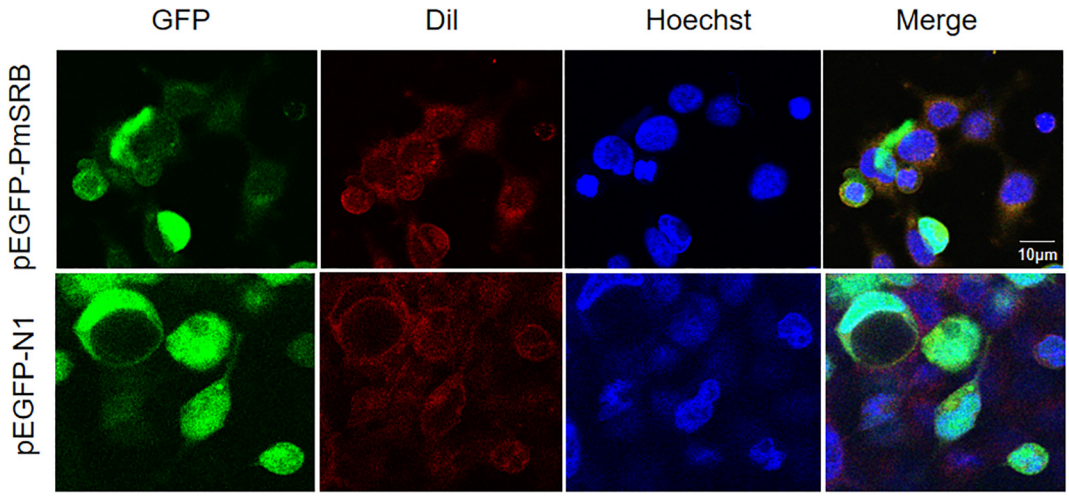

Fig. 5. Subcellular localization of PmSRB in HEK293T cells. Intracellular localization of PmSRB by fluorescence microscopy, 293T cells were transfected with pEGFP-PmSRB (upper row) or pEGFP-N1 (lower row). Localization of nucleus and cytomembrane are shown via Hoechst and Dil staining, respectively.

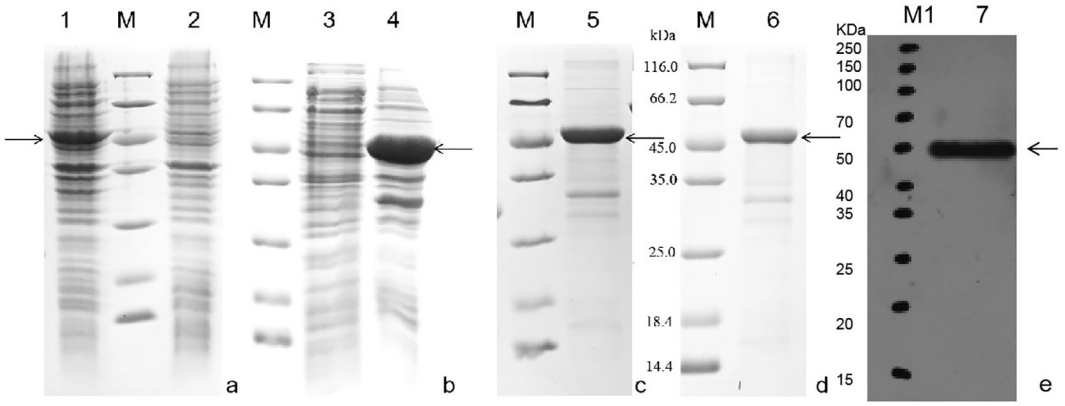

Fig. 6. Expression, purification and western blot analysis of rPmSRB protein. (a) Recombinant expressed protein from *E. coli*. (b) Induced rPmSRB proteins were released from *E. coli* by sonication. (c) Purified rPmSRB proteins from inclusion body. (d) SDS–PAGE of refolded rPmSRB. (e) Western blotting analysis of purified rPmSRB. Lane 1, induced cell-transformed recombinant of PmSRB; lane 2, non-induced cell-transfected recombinant of PmSRB; Lane 3, proteins in supernatant; lane 4, proteins in inclusion body; lane 5, purified rPmSRB; lane 6, rPmSRB after renaturation; lane 7, purified rPmSRB with a 6 × His tag; lane M (26610, Thermo Scientific, USA) and M1 (P12103, helix, China) are the molecular mass standard. rPmSRB is indicated by arrow.

variety of species (Fig. 2), which suggested CD36 domain may play an important role in the long evolutionary process. Generally, the CD36 domain is responsible for ligand binding [8]. In mammals, the amino-terminus of CD36 is substantially shorter than the carboxyl-terminal tail, which is thought to be the site of signal transduction [33]. The presence of a putative CD36 domain in PmSRB suggests that it could act as a scavenger receptor to bind ligands. N-glycosylation consensus sites (e.g., Asn-Xaa-Ser/Thr) are another common feature of scavenger receptor family genes.

The number of N-linked glycosylation sites is various in varied species. In mammal, turtle, chicken and fish, 6–11 N-linked glycosylation sites were detected [34,35]. 7 and 9 N-linked glycosylation sites were detected in crab *Portunus trituberculatus* and sea cucumber *Apostichopus japonicus* [36,37], respectively. In this study, four N-linked glycosylation sites were detected in PmSRB. N-glycosylation is a common post-translational modification that mediates protein synthesis, metabolism and function [38]. N-linked glycosylation in SRB can influence the intracellular transport and lipid-transporter activity. When two N-linked glycosylation sites (Asn-108 or Asn-173) in SR-BI of murine were mutated, the protein failed to locate to the plasma membrane and has a marked reduction in the ability to transfer lipid from HDL to cells [39]. In human CD36, glycosylation is necessary for trafficking to the plasma membrane [40]. However, no individual sit was found to be necessary for surface expression and ligand binding. The double mutant (N102Q-N143Q and N143Q-N184Q) of N-glycosylation in human SR-AI decrease its activity on oligomeric amyloid-βpeptide internalization [41]. It is unclear whether N-linked glycosylation site in PmSRB could influence the ability to bind astaxanthin. Further experimental work will be required to test.

In the current study, two transmembrane domains located in the N- and C-terminals have been reported in many CD36 family proteins from varied species. However, the existence of the N-terminal transmembrane region has been a matter of debate [42]. Some SRB1 proteins are similarly predicted to have single- or double-pass transmembrane structures at various ratios [4]. For example, the predicted rates for the existence of two or one transmembrane domains in the human SRB1 protein are 32% and 68%, respectively. In contrast, the predicted rates of two or one transmembrane domains in the mouse SRB1 protein are 35% and 65%, respectively. In addition, the cytoplasmic C-terminus and C-terminal trans-membrane region of human CD36 protein may be lacked because of some mutations (T1264G and G1439C), which may influence susceptibility to mild malaria cases [43]. In this

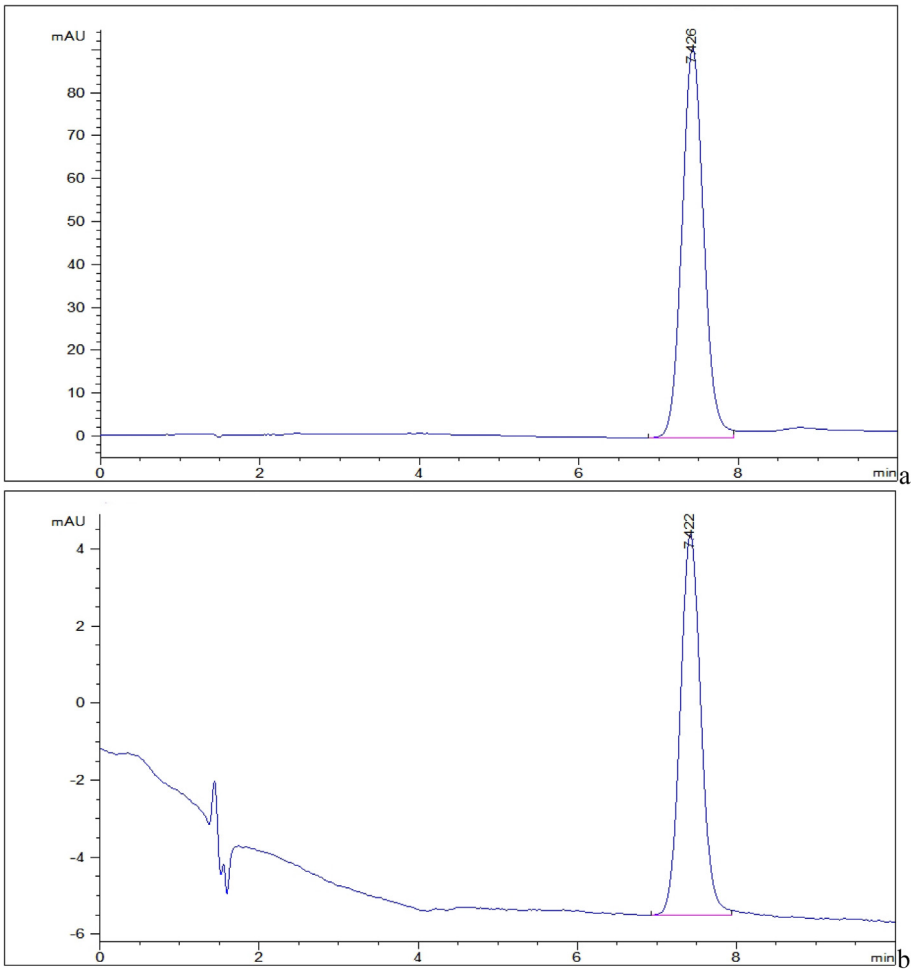

Fig. 7. *In vitro* ligand binding assay of PmSRB. a. Astaxanthin standard; b. As-rPmSRB complex.

study, only one transmembrane region located at the N-terminal was predicted for PmSRB. However, another two SRBs, screened from the transcriptome of *P. monodon* in our lab, demonstrated the existence of two transmembrane domains. In *L. vannamei*, two croquemort gene (named *Lvcroquemort* and *Lvcroquemort-S1*) were identified and characterized [44]. The Lvcroquemort-S1 loses the cytoplasmic C-terminus and C-terminal trans-membrane region [44]. However, the expression of *Lvcroquemort-S1* post immune challenge was increased [44]. It is unclear whether the loss of C-terminal transmembrane region could influence the role of Lvcroquemort-S1 [44].

Based on the SR proteins (SRA, SRB, SRC, and croquemort) and their homologues from many species, we constructed a phylogenetic tree. Results showed that all species belonging to the same class were clustered together. Thus, the phylogenetic tree relationships corresponded to the taxonomic classifications. PmSRB belongs to a subgroup of SRBs. Here, *PmSRB* mRNA was expressed at a high level in the brain and lymphoid organ. Previous studies have also found SRB to be highly expressed in the brains of mammals, fish, and kuruma shrimp [35,44,45]. SRBs are expressed by astrocytes and vascular smooth muscle cells in normal adult mouse and human brains, suggesting that SRBs may mediate interactions between astrocytes or smooth muscle cells and fibrillar beta-amyloid protein [45]. Neurons and glia are enriched in normal brains. Both express SRBs to bind to lipoproteins, such as apoE [46]. SR-B1, which is regulated by hormonal and nutritional stimuli in murine brains [47]. However, the function of SRBs in shrimp remains unclear, although previous studies have indicated that SRBs may be involved in the innate immune system in crustaceans [27]. In this study, similarly, PmSRB was highly expressed in the lymphoid organ, which is a major site for the elimination of pathogens in shrimp [48].

SRBs and related homologs have been implicated as mediators of carotenoid uptake in fruit flies (*D. melanogaster*), silkworms (*B. mori*), birds (*Serinus canaria*), mice, and humans [13,14,16,49,50]. Mutation of a single nucleotide in canary SRB1 results in the recessive white phenotype [14]. In *Drosophila*, mutation of SRB1 can hinder cellular uptake of carotenoids, resulting in blindness [16]. In addition, feeding experiments on silkworm larvae have indicated that Cameo2 (a CD36 family member) has specificity for astaxanthin binding [13]. However, whether SRB can bind to astaxanthin is not fully clear. Previous study on Atlantic salmon identified a novel paralog of SRB1 (i.e., SCARB1) in a region containing a putative QTL for flesh color [17]. However, the functional role for SCARB1 in pigmentation remains unknown. In this study, binding assay and HPLC analysis confirmed that PmSRB can bind to astaxanthin *in vitro*, suggesting that PmSRB may be an important mediator of astaxanthin uptake in shrimp. When astaxanthin binds with protein, its absorbance or peak value will be changed. To date, only a few studies have reported on protein and astaxanthin binding in shrimp. For example, Yang et al. [26] incubated a recombinant lipocalin protein from *M. rosenbergii* with astaxanthin and found that 1 mol of lipocalin could bind to 0.29 mol of astaxanthin. In the current study, the astaxanthin to PmSRB binding ratio was 1:0.48.

However, this does not mean that the binding capacity of SRB is stronger than that of lipocalin. Non-properly folded recombinant proteins cannot bind to astaxanthin, which can influence the binding ratio. Ferrari et al. [51] obtained and incubated two recombinant proteins of crustacyanin subunits H1 and H2 from the American lobster (*Homarus americanus*) with astaxanthin, then analyzed the protein solutions for absorption spectra. Their results indicated that H1 and H2 with astaxanthin replicated the 85–95-nm bathochromic shift found in *H. gammarus* crustacyanin subunits in complex with astaxanthin. In Atlantic salmon, purified α-actinin protein can bind to astaxanthin at a molar ratio of 1.11:1.00 [52]. Though these reports suggest a binding ability of protein to astaxanthin, further study is required to determine details such as binding sites, spatial structures, and binding conditions.

5. Conclusion

In conclusion, in the present study, *PmSRB* was identified and characterized in *P. monodon*. Transcription levels showed that *PmSRB* was highly expressed in the brain and lymphoid organ. The PmSRB protein was purified and could bind to astaxanthin *in vitro*. Furthermore, PmSRB was found in the cell membrane. However, the roles of *PmSRB* are not fully known and thus further investigations are required.

Financial support

This work was funded by Special Fund for National Key R&D Program of China (2018YFD0900103), the Guangdong Marine economy promotion projects (MEPP) Fund (GDOE[2019]A24), Central Public-interest Scientific Institution Basal Research Fund, CAFS (2018HY-ZD0204), Central Public interest Scientific Institution Basal Research Fund, South China Sea Fisheries Research Institute, CAFS (No. 2019TS11), Hainan Provincial Natural Science Foundation of China (319QN335), Guangxi Key Laboratory of Beibu Gulf Marine Biodiversity Conservation, Beibu Gulf University (2019 KB02).

Conflict of interest

The authors declare no conflict of interest.

References

[1] Cheng D, Zhang Y, Liu H, et al. An improving method for extracting total carotenoids in an aquatic animal *Chlamys nobilis*. Food Chem 2019;280:45–50. https://doi.org/10.1016/j.foodchem.2018.12.043. PMid: 30642505.
[2] Von Lintig J. Colors with functions: elucidating the biochemical and molecular basis of carotenoid metabolism. Annu Rev Nutr 2010;30:35–56. https://doi.org/10.1146/annurev-nutr-080508-141027. PMid: 20415581.
[3] Toews D, Hofmeister NR, Taylor SA. The evolution and genetics of carotenoid processing in animals. Trends genet 2017;33(3):171–82. https://doi.org/10.1016/j.tig.2017.01.002. PMid: 28174022.
[4] Sakudoh T, Iizuka T, Narukawa J, et al. A CD36-related transmembrane protein is coordinated with an intracellular lipid-binding protein in selective carotenoid transport for cocoon coloration. J biol chem 2010;285 (10):7739–51. https://doi.org/10.1074/jbc.M109.074435. PMid: 20053988.
[5] Nicholas MW, Jacques G, Brett DG. A review of carotenoid utilisation and function in crutacean aquculture. Rev Aquacult 2017;9:141–56. https://doi.org/10.1111/raq.12109.
[6] Sakudoh T, Kuwazaki S, Iizuka T, et al. CD36 homolog divergence is responsible for the selectivity of carotenoid species migration to the silk gland of the silkworm *Bombyx mori*. J lipid res 2013;54(2):482–95. https://doi.org/10.1194/jlr.M032771. PMid: 23160179.
[7] Bhosale P, Larson AJ, Frederick JM, et al. Identification and characterization of a Pi isoform of glutathione S-transferase (GSTP1) as a zeaxanthin-binding protein in the macula of the human eye. J Biol Chem 2004;279:49447–54. https://doi.org/10.1074/jbc.M405334200. PMid: 15355982.
[8] Canton J, Neculai D, Grinstein S. Scavenger receptors in homeostasis and immunity. Nat rev Immunol 2013;13(9):621–34. https://doi.org/10.1038/nri3515. PMid: 23928573.
[9] Zani IA, Stephen SL, Mughal NA, et al. Scavenger receptor structure and function in health and disease. Cells 2015;4(2):178–201. https://doi.org/10.3390/cells4020178. PMid: 26010753.
[10] PrabhuDas MR, Baldwin CL, Bollyky PL, et al. A consensus definitive classification of scavenger receptors and their roles in health and disease. J Immunol 2017;198(10):3775–89. https://doi.org/10.4049/jimmunol.1700373. PMid: 28483986.
[11] Khush RS, Lemaitre B. Genes that fight infection: what the *Drosophila* genome says about animal immunity. Trends genet 2000;16(10):442–9. https://doi.org/10.1016/S0168-9525(00)02095-3.
[12] Shyam R, Vachali P, Gorusupudi A, et al. All three human scavenger receptor class B proteins can bind and transport all three macular xanthophyll carotenoids. Arch Biochem Biophys 2017;634:21–8. https://doi.org/10.1016/j.abb.2017.09.013. PMid: 28947101.
[13] Tsuchida K, Sakudoh T. Recent progress in molecular genetic studies on the carotenoid transport system using cocoon-color mutants of the silkworm. Arch Biochem Biophys 2015;572:151–7. https://doi.org/10.1016/j.abb.2014.12.029. PMid: 25579881.
[14] Toomey MB, Lopes RJ, Araújo PM, et al. High-density lipoprotein receptor SCARB1 is required for carotenoid coloration in birds. Proc Natl Acad Sci USA 2017;114(20):5219–24. https://doi.org/10.1073/pnas.1700751114. PMid: 28465440.
[15] Liu H, Zheng H, Zhang H, et al. A *de novo* transcriptome of the noble scallop, *Chlamys nobilis*, focusing on mining transcripts for carotenoid-based coloration. BMC Genomics 2015;16(1):44. https://doi.org/10.1186/s12864-015-1241-x. PMid: 25651863.
[16] Kiefer C, Sumser E, Wernet MF, et al. A class B scavenger receptor mediates the cellular uptake of carotenoids in *Drosophila*. P Natl Acad Sci USA 2002;99 (16):10581–6. https://doi.org/10.1073/pnas.162182899. PMid: 12136129.
[17] Sundvold H, Helgeland H, Baranski M, et al. Characterisation of a novel paralog of scavenger receptor class B member I (SCARB1) in Atlantic salmon (*Salmo salar*). BMC Genet 2011;12:52. https://doi.org/10.1186/1471-2156-12-52. PMid: 21619714.
[18] Lei C, Hao RJ, Zheng Z, et al. Molecular cloning and characterisation of scavenger receptor class B in pearl oyster *Pinctada fuctada martensii*. Electron J Biotechn 2017;30:12–7. https://doi.org/10.1016/j.ejbt.2017.08.003.
[19] Ambati RR, Phang SM, Ravi S, et al. Astaxanthin: sources, extraction, stability, biological activities and its commercial applications-a review. Mar Drugs 2014;12(1):128–52. https://doi.org/10.3390/md12010128. PMid: 24402174.
[20] Britton G. Functions of intact carotenoids. In: Britton G,Liaaen-Jensen S, Pfander H (eds) Carotenoids. Natural Functions 2008;4:189–212. Birkhauser Verlag AG, Basel. 10.1007/978-3-7643-7499-0_10.
[21] Su F, Huang B, Liu JG. The carotenoids of shrimps (Decapoda: Caridea and Dendrobranchiata) cultured in China. J Crustacean Biol 2018;38(5):523–30. https://doi.org/10.1093/jcbiol/ruy049.
[22] Zhang C, Su F, Li S, et al. Isolation and identification of the main carotenoid pigment from a new variety of the ridgetail white prawn *Exopalaemon carinicauda*. Food Chem 2018;269:450–4. https://doi.org/10.1016/j.foodchem.2018.06.143. PMid: 30100459.
[23] Chayen NE, Cianci M, Grossmann JG, et al. Unravelling the structural chemistry of the colouration mechanism in lobster shell. Acta Crystallogr D, Biol Crystallogr 2003;59(12):2072–82. https://doi.org/10.1107/S0907444903025952. PMid: 14646064.
[24] Budd AM, Hinton TM, Tonks M, et al. Rapid expansion of pigmentation genes in penaeid shrimp with absolute preservation of function. J Exp Biol 2017;220 (22):4109–18. https://doi.org/10.1242/jeb.164988. PMid: 28851818.
[25] Ertl NG, Elizur A, Brooks P, et al. Molecular characterisation of colour formation in the prawn *Fenneropenaeus merguiensis*. PLoS ONE 2013;8(2):. https://doi.org/10.1371/journal.pone.0056920. PMid: 23441225e56920.
[26] Yang F, Wang MR, Ma YG, et al. Prawn lipocalin: characterization of a color shift induced by gene knockdown and ligand binding assay. J exp zool Part A 2011;315(9):562–71. https://doi.org/10.1002/jez.706. PMid: 21905240.
[27] Kong T, Gong Y, Liu Y, et al. Scavenger receptor B promotes bacteria clearance by enhancing phagocytosis and attenuates white spot syndrome virus proliferation in *Scylla paramamosian*. Fish shellfish immun 2018;78:79–90. https://doi.org/10.1016/j.fsi.2018.04.027. PMid: 29679762.
[28] Hou F, Liu T, Wang Q, et al. Identification and characterization of two Croquemort homologues in penaeid shrimp *Litopenaeus vannamei*. Fish Shellfish Immunol 2017;60:1–5. https://doi.org/10.1016/j.fsi.2016.09.047. PMid: 27670083.
[29] FAO. 2019. FAO yearbook. Fishery and Aquaculture Statistics 2017,PP12,30.
[30] Torrissen OJ. Pigmentation of salmonids: interactions of astaxanthin and canthaxanthin on pigment deposition in rainbow-trout. Aquaculture 1989;79:363–73. https://doi.org/10.1016/0044-8486(89)90478-X.
[31] Livak KJ, Schmittge TD. Analysis of relative gene expression data using real-time quantitative PCR and the $^{2-\Delta\Delta}_{C}$T Method. Methods 2001;25(4):402–8. https://doi.org/10.1006/meth.2001.1262. PMid: 11846609.
[32] Wu YM, Yang L, Li XJ, et al. A class B scavenger receptor from *Eriocheir sinensis* (EsSR-B1) restricts bacteria proliferation by promoting phagocytosis. Fish Shellfish Immunol 2017;70:426–36. https://doi.org/10.1016/j.fsi.2017.09.034. PMid: 28916359.
[33] Rahaman SO, Lennon DJ, Febbraio M, et al. A CD36-dependent signaling cascade is necessary for macrophage foam cell formation. Cell Metab 2006;4 (3):211–21. https://doi.org/10.1016/j.cmet.2006.06.007. PMid: 16950138.
[34] Yang D, Han Y, Chen L, et al. Scavenger receptor class B type I (SR-BI) in *Ruditapes philippinarum*: A versatile receptor with multiple functions. Fish

Shellfish Immunol. 2019;88:328–34. https://doi.org/10.1016/j.fsi.2019.03.009. PMid: 30858096.
[35] Ou M, Huang R, Luo Q, et al. Characterisation of scavenger receptor class B type 1 in rare minnow (*Gobiocypris rarus*). Fish Shellfish Immunol 2019;89:614–22. https://doi.org/10.1016/j.fsi.2019.04.031. PMid: 30991152.
[36] Yang N, Zhang DF, Tao Z, et al. Identification of a novel class B scavenger receptor homologue in *Portunus trituberculatus*: Molecular cloning and microbial ligand binding. Fish Shellfish Immun 2016;58:73–81. https://doi.org/10.1016/j.fsi.2016.09.023. PMid: 27633673.
[37] Che Z, Shao Y, Zhang W, et al. Cloning and functional analysis of scavenger receptor B gene from the sea cucumber *Apostichopus japonicus*. Dev Comp Immunol. 2019;99:. https://doi.org/10.1016/j.dci.2019.103404. PMid: 31152761103404.
[38] Varki A. Biological roles of glycans. Glycobiology 2017;27(1):3–49. https://doi.org/10.1093/glycob/cww086. PMid: 27558841.
[39] Viñals M, Xu S, Vasile E, et al. Identification of the n-linked glycosylation sites on the high density lipoprotein (HDL) receptor SR-BI and assessment of the effects on HDL binding and selective lipid uptake. J Biol Chem 2003;278:5325–32. https://doi.org/10.1074/jbc.M211073200. PMid: 12429731.
[40] Hoosdally SJ, Andress EJ, Wooding C, et al. The human scavenger receptor CD36: glycosylation status and its role in trafficking and function. J Biol Chem 2009;284:16277–88. https://doi.org/10.1074/jbc.M109.007849. PMid: 19369259.
[41] Tsay HJ, Huang YC, Chen YJ, et al. Identifying N-linked glycan moiety and motifs in the cysteine-rich domain critical for N-glycosylation and intracellular trafficking of SR-AI and MARCO. J Biomed Sci 2016;23:27. https://doi.org/10.1186/s12929-016-0244-5. PMid: 26892079.
[42] Gruarin P, Thorne RF, Dorahy DJ, et al. CD36 is a ditopic glycoprotein with the N-terminal domain implicated in intracellular transport. Biochem Biophys Res Commun 2000;275(2):446–54. https://doi.org/10.1006/bbrc.2000.3333. PMid: 10964685.
[43] Aitman TJ, Cooper LD, Norsworthy PJ, et al. Malaria susceptibility and CD36 mutation. Nature 2000;405(6790):1015–6. https://doi.org/10.1038/35016636. PMid: 10890433.
[44] Mekata T, Okugawa S, Inada M, et al. Class B scavenger receptor, Croquemort from kuruma shrimp *Marsupenaeus japonicus*: Molecular cloning and characterization. Mol Cell Probe 2011;25(2–3):94–100. https://doi.org/10.1016/j.mcp.2011.02.001. PMid: 21324353.
[45] Husemann J, Silverstein SC. Expression of scavenger receptor class B, type I, by astrocytes and vascular smooth muscle cells in normal adult mouse and human brain and in Alzheimer's disease brain. Am J Clin Pathol 2001;158 (3):825–32. https://doi.org/10.1016/S0002-9440(10)64030-8.
[46] Arai T, Rinninger F, Varban L, et al. Decreased selective uptake of high density lipoprotein cholesteryl esters in apolipoprotein E knock-out mice. Proc Natl Acad Sci USA 1999;96(21):12050–5. https://doi.org/10.1073/pnas.96.21.12050. PMid: 10518574.
[47] Srivastava RA. Scavenger receptor class B type I expression in murine brain and regulation by estrogen and dietary cholesterol. J Neurol Sci 2003;210(1–2):11–8. https://doi.org/10.1016/S0022-510X(03)00006-6.
[48] van de Braak CB, Botterblom MH, Taverne N, et al. The roles of haemocytes and the lymphoid organ in the clearance of injected Vibrio bacteria in *Penaeus monodon* shrimp. Fish Shellfish Immunol 2002;13(4):293–309. https://doi.org/10.1006/fsim.2002.0409. PMid: 12443012.
[49] During A, Harrison EH. Mechanisms of provitamin A (carotenoid) and vitamin A (retinol) transport into and out of intestinal Caco-2 cells. J lipid res 2007;48 (10):2283–94. https://doi.org/10.1194/jlr.M700263-JLR200. PMid: 17644776.
[50] Borel P, Lietz G, Goncalves A, et al. CD36 and SR-BI are involved in cellular uptake of provitamin A carotenoids by Caco-2 and HEK cells, and some of their genetic variants are associated with plasma concentrations of these micronutrients in humans. J Nutr 2013;143(4):448–56. https://doi.org/10.3945/jn.112.172734. PMid: 23427331.
[51] Ferrari M, Folli C, Pincolini E, et al. Structural characterization of recombinant crustacyanin subunits from the lobster *Homarus americanus*. Acta Cryst 2012;68(8):846–53. https://doi.org/10.1107/S1744309112026103. PMid: 22869108.
[52] Matthews SJ, Ross NW, Lall SP, et al. Astaxanthin binding protein in Atlantic salmon. Comp Biochem Phys B 2006;144(2):206–14. https://doi.org/10.1016/j.cbpb.2006.02.007. PMid: 16644255.